COMU: A Safer and More Effective Replacement for Benzotriazole-Based Uronium Coupling Reagents**

Ayman El-Faham,*[a, b, c] Ramon Subirós Funosas,[a, d] Rafel Prohens,[e] and Fernando Albericio*[a, d, f]

Abstract: We describe a new family of uronium-type coupling reagents that differ in their iminium moieties and leaving groups. The presence of the morpholino group in conjunction with an oxime derivative—especially ethyl 2-cyano-2-(hydroxyimino)acetate (Oxyma)—had a marked influence on the solubilities, stabilities, and reactivities of the reagents. Finally, the new uronium salt derived from Oxyma (COMU) performed extremely well in the presence of only 1 equiv of base, thereby confirming the effect of the hydrogen bond acceptor in the reaction. COMU also showed a less hazardous safety profile than the benzotriazole-based HDMA and HDMB, which exhibited unpredictable autocatalytic decompositions. Furthermore, the Oxyma moiety contained in COMU suggests a lower risk of explosion than in the case of the benzotriazole derivatives.

Keywords: coupling reagents · Oxyma · peptides · solid-phase synthesis · uronium salts

Introduction

Peptide synthesis is based on an appropriate combination of protecting groups and a suitable choice of coupling

[a] Prof. A. El-Faham, R. S. Funosas, Prof. F. Albericio
Institute for Research in Biomedicine, Barcelona Science Park
Baldiri Reixac 10, 08028 Barcelona (Spain)
Fax: (+34) 93-403-71-26
E-mail: aymanel_faham@hotmail.com
        albericio@irbbarcelona.org

[b] Prof. A. El-Faham
Department of Chemistry, College of Science
King Saud University, P.O. Box 2455
Riyadh 11451 (Saudi Arabia)

[c] Prof. A. El-Faham
Department of Chemistry, Faculty of Science
Alexandria University, Ibrahimia 21321, Alexandria (Egypt)

[d] R. S. Funosas, Prof. F. Albericio
CIBER-BBN, Networking Centre on Bioengineering
Biomaterials and Nanomedicine, Barcelona Science Park
Baldiri Reixac 10, 08028 Barcelona (Spain)

[e] R. Prohens
Plataforma de Polimorfisme i Calorimetria
Serveis Cientificotècnics, University of Barcelona
Barcelona Science Park, Baldiri Reixac 10, 08028 Barcelona (Spain)

[f] Prof. F. Albericio
Department of Organic Chemistry, University of Barcelona
Martí i Franqués 1–11, 08028 Barcelona (Spain)

[**] All abbreviations used in the text are given in reference [1].

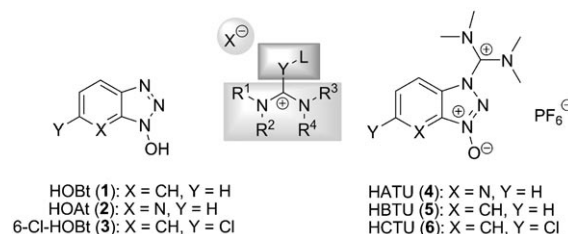📖 Supporting information for this article is available on the WWW under http://dx.doi.org/10.1002/chem.200900615.

method.[1] Nowadays, almost all peptide bonds are formed in the presence of 1-hydroxybenzotriazole (HOBt, **1**, Figure 1, left)[2] or its derivatives (HOAt, **2**; 6-Cl-HOBt,

Figure 1. General structures of HOBt derivatives (left), immonium/uronium salts (center), and the most commonly used immonium salts (right).

3).[3,4] HOBt derivatives are therefore either used in combination with a carbodiimide or another coupling agent or are built into a stand-alone reagent such as an immonium [HATU (**4**), HBTU (**5**), HCTU, (**6**), Figure 1, right] or phosphonium (PyAOP, PyBOP, PyClock) salt.[5,6] An onium salt consists of two parts: a leaving group (YL) and the iminium moiety (Figure 1, center).

Recently we showed that the incorporation of a hydrogen bond acceptor in the iminium part resulted in performances superior to those described previously.[7] As reported in our previous work, the presence of an oxygen in the iminium

These are not the final page numbers! ⟀⟀

moiety confers more solubility on the reagent, enhances coupling yields, and decreases racemization, thereby allowing the use of just 1 equiv of base. HDMA (**7**), HDMB (**8**), and 6-HDMCB (**9**) are thus more efficient in terms of coupling efficiency and reduction of racemization than their counterparts HATU (**4**), HBTU (**5**), and HCTU (**6**). Importantly, 6-HDMCB (**9**), which is consistently superior to HDMB (**8**), often performs in a similar manner to HATU (**4**), which is one of the most powerful commercially available immonium coupling reagents known to date.[7] It is important to note that all these reagents exist in their *N*-forms,[8] which are less reactive than the *O*-forms (Figure 2).[9]

HDMA (**7**): X = N, Y = H
HDMB (**8**): X = CH, Y = H
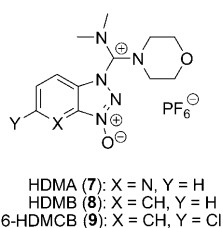6-HDMCB (**9**): X = CH, Y = Cl

Figure 2. General structures of the dimethyl-morpholino immonium salts, which are superior to their tetramethyl counterparts.

Recent reports have confirmed the explosive properties of HOBt derivatives.[10] In our preceding paper,[11] we showed that Oxyma (**10**, Figure 3) is an excellent replacement for HOBt and its analogues. Here we report a new uronium salt, COMU (**11**, Figure 3), which represents the combination of a morpholonium-based immonium moiety, introduced in our previous work, and Oxyma (**10**) as leaving group, as a superior and safe coupling reagent for amide formation.

Results and Discussion

Scheme 1 shows the uronium salts prepared for the first screening. We tested four distinct oximes (**17a–d**) and several iminium moieties, including dimethyl-morpholino, pyrrolidino-morpholino, and dimethyl-pyrrolidino systems, the last of these as a reference for the role of the pyrrolidino moiety. The corresponding unsymmetrical uronium salts were prepared by treating *N,N*-dialkyl carbamoyl
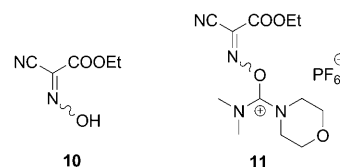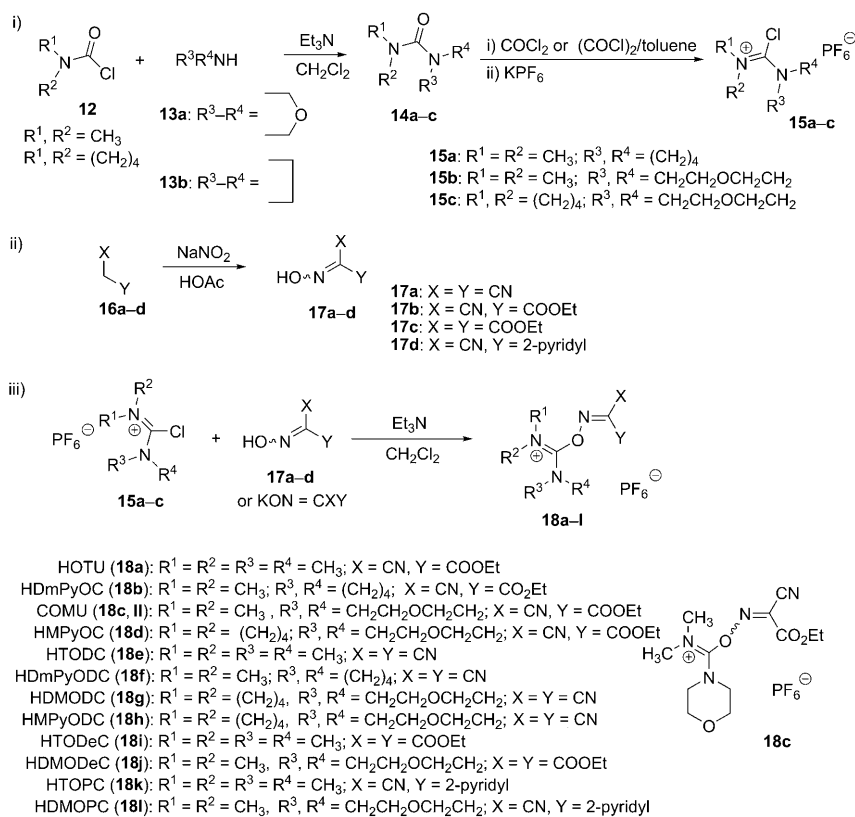
Figure 3. Structures of Oxyma and the new uronium salt.

chlorides **12a** or **12b** with morpholine (**13a**) or pyrrolidine (**13b**) to give the urea derivatives **14a–c** (Scheme 1). Urea derivatives (**14a–c**) were treated with phosgene or oxalyl chloride to yield the corresponding chloro salts, which were stabilized by the formation of hexafluorophosphate salts (**15a–c**). Subsequent treatment with oxime derivatives (**17a–d**), obtained by nitrosation from the active methylene compounds **16a–d**, in the form of their potassium salts or in the presence of Et$_3$N provided the target compounds (**18a–l**, Scheme 1).

Interestingly, the ^{13}C NMR spectra of these compounds indicated displacements of the carbocationic carbon of 156.11 ppm for HOTU (**18a**, the hexafluorophosphate counterpart of TOTU, already described in the literature)[12] and 156.14 ppm for COMU (**18c**). These displacements are consistent with those reported for this kind of compound in the *O*-form.[13,9] X-ray crystallography confirmed this hypothesis (Figure 4).

HOTU (**18a**): R^1 = R^2 = R^3 = R^4 = CH$_3$; X = CN, Y = COOEt
HDmPyOC (**18b**): R^1 = R^2 = CH$_3$; R^3, R^4 = (CH$_2$)$_4$; X = CN, Y = CO$_2$Et
COMU (**18c, II**): R^1 = R^2 = CH$_3$, R^3, R^4 = CH$_2$CH$_2$OCH$_2$CH$_2$; X = CN, Y = COOEt
HMPyOC (**18d**): R^1 = R^2 = (CH$_2$)$_4$; R^3, R^4 = CH$_2$CH$_2$OCH$_2$CH$_2$; X = CN, Y = COOEt
HTODC (**18e**): R^1 = R^2 = R^3 = R^4 = CH$_3$; X = Y = CN
HDmPyODC (**18f**): R^1 = R^2 = CH$_3$; R^3, R^4 = (CH$_2$)$_4$; X = Y = CN
HDMODC (**18g**): R^1 = R^2 = (CH$_2$)$_4$, R^3, R^4 = CH$_2$CH$_2$OCH$_2$CH$_2$; X = Y = CN
HMPyODC (**18h**): R^1 = R^2 = (CH$_2$)$_4$, R^3, R^4 = CH$_2$CH$_2$OCH$_2$CH$_2$; X = Y = CN
HTODeC (**18i**): R^1 = R^2 = R^3 = R^4 = CH$_3$; X = Y = COOEt
HDMODeC (**18j**): R^1 = R^2 = CH$_3$, R^3, R^4 = CH$_2$CH$_2$OCH$_2$CH$_2$; X = Y = COOEt
HTOPC (**18k**): R^1 = R^2 = R^3 = R^4 = CH$_3$; X = CN, Y = 2-pyridyl
HDMOPC (**18l**): R^1 = R^2 = CH$_3$, R^3, R^4 = CH$_2$CH$_2$OCH$_2$CH$_2$; X = CN, Y = 2-pyridyl

Scheme 1. Procedure followed for the preparation of the oxime-based uronium-type coupling reagents.
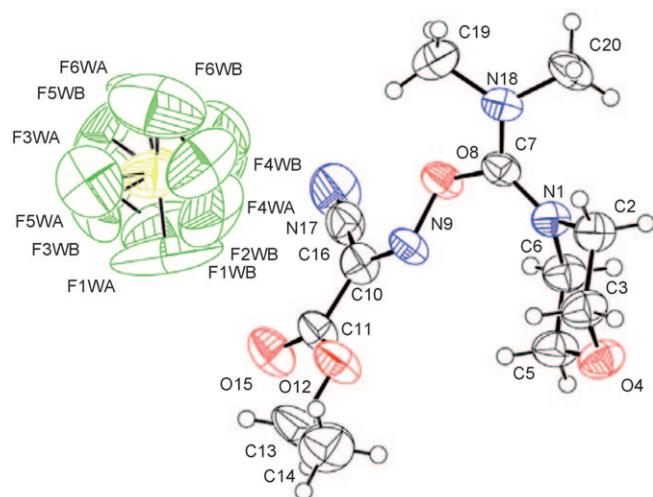
Figure 4. X-ray crystallographic structure of COMU.

To determine the compatibilities of the new coupling reagents with peptide synthesis in both manual and automatic modes, their solubilities and stabilities in solution and in the solid state were examined by ^{1}H NMR analysis. The presence of the oxygen in the iminium structure increased the stabilities of the coupling reagent relative to their tetramethyl derivatives (entries 3 vs. 4, Table 1). Furthermore, Oxyma

Table 1. Hydrolytic stabilities [%] of immonium/uronium-type coupling reagents in DMF (open vials).

Entry	Coupling reagent	5 h [%]	24 h [%]	48 h [%]
1	HATU (**4**)	99	95	76
2	HBTU (**5**)	100	98	86
3	HOTU (**18a**)	100	95	84
4	COMU (**18c**)	100	100	93

derivatives have greater stabilities than the benzotriazole derivatives HATU (**4**) and HBTU (**5**) (Figure 1). All these reagents showed stabilities greater than 95% in a closed vial. These observations are of practical relevance for both solid-phase and solution strategies: when the activation of a carboxylic acid is slow and the coupling reagent is not stable, it is degraded and no longer able to activate the carboxylic function. This feature is crucial in cyclization steps or for segment coupling steps in convergent strategies, in which the excess of the carboxylic function is either absent (cyclization) or low (segment coupling) and couplings are therefore very slow.

Table 2 indicates that the presence of the oxygen atom in the carbon skeleton and the leaving group are of marked relevance for the solubilities of the compounds. Thus, all dimethyl-morpholino derivatives (**18c**, **18g**, and **18l**) were more soluble than their tetramethyl counterparts (**18a**, **18e**, and **18k**) (Table 2, entries 3 vs. 4, 5 vs. 6, and 7 vs. 8). Furthermore, ethyl 2-cyano-2-(hydroxyimino)acetate (Oxyma, **10**) derivatives were more soluble than dicyano and cyanopyridinyl ones (Table 2, entries 3, 4 vs. 5, 6 and 7, 8). Thus,

Table 2. Effect of oxygen on the solubility of the immonium-/uronium-type coupling reagents in DMF.

Entry	Coupling reagent	Wt/1 mL	Molarity
1	HATU (**4**)	0.165	0.43
2	HBTU (**5**)	0.175	0.46
3	HOTU (**18a**)	0.420	1.09
4	COMU (**18c**)	0.620	1.44
5	HTODC (**18e**)	0.410	1.20
6	HDMODC (**18g**)	0.520	1.36
7	HTOPC (**18k**)	0.320	0.79
8	HDMOPC (**18l**)	0.430	0.98

COMU (**18c**) and HDMODC (**18g**) were the most soluble. They were used to prepare solutions of up to 1.5 M and showed clearly higher solubilities than the benzotriazole derivatives **4** and **5** (Table 2, entries 4, 6 vs. 1, 2). This increased solubility can be used to prepare more concentrated solutions in order to enhance coupling yields and to facilitate the removal of the excess of coupling reagent and the urea side-products during the workup in a solution-mode approach.

A further characteristic of the Oxyma derivative **18c** is that the course of reaction can be followed due to a change in color, which depends on the type of base used. Thus, 2 min after the addition of the coupling reagent, a solution of **18c** has turned orange-red when DIEA is used as a base, and pink in the case of TMP. Once the reaction is complete, the solutions become colorless and yellow, respectively (Figure 5).

Figure 5. A) 2 min after the addition of COMU (pink with TMP and orange-red with DIEA). B) 1 h after the addition of COMU.

A preliminary screening on the efficiency of Oxyma-based coupling reagents **18a** and **18c**, in the coupling of hindered amino acids, was examined with two model systems (Fmoc-Val-OH + H-Val-NH$_2$ and Z-Aib-OH + H-Val-OMe) in solution. The reaction mixtures were followed by HPLC; the t_R values for the starting Fmoc-Val-OH and Z-Aib-OH were 20.89 min and 18.25 min, respectively, and those for the products (Fmoc-Val-Val-NH$_2$ and Z-Aib-Val-

These are not the final page numbers! ↗↗

OMe) were 19.88 min and 20.90 min, respectively. The Oxyma-based coupling reagents were more reactive than the benzotriazole derivatives (Tables 3 and 4, **18c**, **18a** vs. **7**,

Table 3. Levels of coupling of Fmoc-Val-Val-NH$_2$ with use of several different coupling reagents and a range of equivalents of DIEA in DMF as a solvent.[a]

time [min]	HATU (**4**) yield [%]		HDMA (**7**) yield [%]		COMU (**18c**) yield [%]		HOTU (**18a**) yield [%]	
	2 equiv	1 equiv	2 equiv	1 equiv	2 equiv	1 equiv	2 equiv	1 equiv
5	83.0	70.0	94.8	80.0	95.1	82.0	85.0	71.0
10	87.6	76.0	95.0	85.0	96.0	86.0	89.0	78.0
20	90.5	80.0	96.4	90.0	98.0	90.1	91.0	83.0
30	92.5	82.0	98.0	93.5	98.5	94.5	93.0	86.0
60	93.0	82.0	99.0	95.5	100.0	96.0	94.0	87.0
120	94.0	83.0	99.0	96.0	100.0	98.0	96.0	88.0

[a] HPLC conditions: linear gradient of 10 to 90% CH$_3$CN/0.1% TFA in H$_2$O/0.1%TFA over 30 min, detection at 200 nm. Flow rate = 1 mL min^{-1} Column: Waters C$_{18}$, 5 μm, 4.6×150 mm (Waters Dual Wavelength Detector and Waters 717 Plus auto sampler). t_R (Fmoc-Val-OH) = 20.89 min, t_R (Fmoc-Val-Val-NH$_2$) = 19.88 min.

Table 4. Levels of coupling of Z-Aib-Val-OMe with use of several different coupling reagents and a range of equivalents of DIEA in DMF as a solvent.[a]

time [min]	HATU (**4**) yield [%]	HBTU (**5**) yield [%]	HDMA (**7**) yield [%]		COMU (**18c**) yield [%]		HOTU (**18a**) yield [%]	
	2 equiv	2 equiv	2 equiv	1 equiv	2 equiv	1 equiv	2 equiv	1 equiv
2	80.0	70.0	89.0	80.5	89.0	85.0	85.0	69.0
5	85.0	76.0	91.0	86.5	92.0	89.0	88.0	74.0
10	87.0	78.0	93.0	88.0	93.0	90.0	89.0	77.0
20	89.0	80.0	94.0	89.5	95.0	91.0	90.0	82.0
30	90.0	81.0	96.0	90.0	97.0	93.0	91.0	86.0
60	91.0	83.0	97.0	91.0	98.0	96.0	91.3	86.0
120	92.0	83.0	98.0	91.0	99.0	97.0	92.0	86.0

[a] HPLC conditions: linear gradient of 10 to 90% CH$_3$CN/0.1% TFA in H$_2$O/0.1%TFA over 30 min, detection at 200 nm, flow rate = 1 mL min^{-1}, Column: Waters C$_{18}$, 5 μm, 4.6×150 mm (Waters Dual Wavelength Detector and Waters 717 Plus auto sampler). t_R (Z-Aib-OH) = 18.25 min, t_R (Z-Aib-Val-OMe) = 20.90 min. t_R (Z-Aib-OAt) = 22.30 min, t_R (Z-Aib-OBt) = 22.80 min, t_R (Z-Aib-Oxyma) = 23.90 min.

4). Again, the morpholine derivatives were superior to their tetramethyl counterparts (Tables 3 and 4, **18c**, **7** vs. **18a**, **4**). In both cases, COMU (**18c**) was superior to HATU (**4**), the most potent of the currently commercially available coupling reagents. This superiority was more remarkable when only 1 equiv of base was used (Table 3 and Table 4), thereby reaffirming the hydrogen bond acceptor role of the oxygen in the morpholino moiety.

Once these encouraging results with the Oxyma-based COMU (**18c**) had been obtained, a deeper study using several oxime derivatives were carried out. Two model peptides, Z-Phg-Pro-NH$_2$ and Z-Phe-Val-Pro-NH$_2$, were used to study the retention of configuration achieved with the new coupling reagents.[7]

The novel uronium coupling reagents were tested and compared with classical immonium salts (including the benzotrizole derivatives **19**, **20**, and **21**, containing pyrrolidino-morpholino systems, Figure 6) with the aid of these models, which involve stepwise and also [2+1] segment coupling (Tables 5 and 6). For the stepwise coupling of Z-Phg-OH to H-Pro-NH$_2$ to produce Z-Phg-Pro-NH$_2$, the oxime-based COMU (**18c**), HOTU (**18a**), HTODC (**18e**), and HDMODC (**18g**) gave better conservation of chirality than the benzotriazole-based HATU (**4**), HBTU (**5**), HDMA (**7**), HDMB (**8**), and 6-HDMCB (**9**) (Table 5).[7] The dimethyl-morpholino derivative COMU (**18c**) induced less racemization than other Oxyma derivatives containing different iminium moieties (**18a**, **18b**, **18d**) and than other uronium salts containing different oxime substituents (**18g**, **18l**). In the oxime series, the worst results were obtained
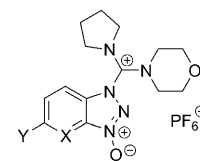
HMPyA (**19**): X = N, Y = H
HMPyB (**20**): X = CH, Y = H
HMPyC (**21**): X = CH, Y = Cl

Figure 6. General structures of benzotriazole-based immonium salts containing pyrrolidino-morpholino systems.

Table 5. Yields and racemization for the formation of Z-Phg-Pro-NH$_2$ in DMF (solution-phase synthesis).[a]

Coupling reagent	Base (equiv)	Yield [%]	D,L [%]
HATU (**4**)	DIEA (2)	78.4	3.1
	TMP (2)	77.9	2.1
	DIEA (1)	74.8	2.4
HBTU (**5**)	DIEA (2)	80.2	8.2
	TMP (2)	81.2	6.4
	DIEA (1)	75.0	5.3
HDMA (**7**)	DIEA (2)	81.2	1.6
	TMP (2)	80.3	3.9
	DIEA (1)	82.3	1.6
HDMB (**8**)	DIEA (2)	80.8	3.8
	TMP (2)	79.9	7.8
	DIEA (1)	82.3	3.1
6-HDMCB (**9**)	DIEA (2)	84.5	1.5
HMPyA (**19**)	DIEA (2)	89.9	2.6
HMPyB (**20**)	DIEA (2)	88.9	4.9
HMPyC (**21**)	DIEA (2)	90.1	2.1
HOTU (**18a**)	DIEA (2)	78.9	0.17
	TMP (2)	90.0	1.20
	TMP (1)	80.3	0.70
COMU (**18c**)	DIEA (2)	88.2	0.12
	TMP (2)	91.0	0.90
	TMP (1)	93.0	0.40
HDmPyOC (**18b**)	DIEA (2)	89.3	0.31
HMPyOC (**18d**)	DIEA (2)	89.8	0.32
HTODC (**18e**)	DIEA (2)	89.3	0.39
HDMODC (**18g**)	DIEA (2)	90.1	0.40
HDmPyODC (**18f**)	DIEA (2)	88.7	0.44
HMPyODC (**18h**)	DIEA (2)	90.2	0.35
HTOPC (**18k**)	DIEA (2)	85.3	28.9
HDMOPC (**18l**)	DIEA (2)	86.0	13.6

[a] LL and DL forms of the test dipeptide are described elsewhere.[7] The t_R values for LL and DL were identified by co-injection with authentic and pure samples of LL. HPLC system: linear gradient of 20 to 50% CH$_3$CN/ 0.1% TFA in H$_2$O/0.1%TFA over 30 min, detection at 200 nm Water Symmetry C$_{18}$ 5 μm 4.6×150 mm, $t_{R\,LL}$ = 26.01 min., $t_{R\,DL}$ = 27.40 min.

FULL PAPER

Table 6. Yields and racemization for the formation of Z-Phe-Val-Pro-NH$_2$ (2+1) in DMF (solution-phase synthesis).[a]

Coupling reagent	Base (equiv)	Yield [%]	LDL [%]
HATU (**4**)	DIEA (2)	85.8	13.9
	DIEA (1)	83.2	11.0
	TMP (2)	78.0	5.3
	TMP (1)	76.1	4.9
HBTU (**5**)	DIEA (2)	89.7	27.7
	DIEA (1)	78.6	16.3
	TMP (2)	81.2	14.2
HDMA (**7**)	DIEA (2)	89.3	10.5
	DIEA (1)	87.4	5.1
	TMP (2)	86.2	3.7
	TMP (1)	84.1	3.8
HDMB (**8**)	DIEA (2)	88.7	20.3
	DIEA (1)	86.3	11.5
	TMP (2)	87.1	13.3
	TMP (1)	80.1	10.5
6-HDMCB (**9**)	DIEA (2)	79.9	13.9
	TMP (2)	80.8	6.5
HMPyA (**19**)	TMP (2)	90.1	4.1
HMPyB (**20**)	TMP (2)	86.8	15.3
HMPyC (**21**)	TMP (2)	89.9	8.7
HOTU (**18a**)	DIEA (2)	91.2	23.6
	TMP (2)	88.7	7.4
	TMP (1)	80.3	7.5
COMU (**18c**)	DIEA (2)	91.3	19.3
	TMP (2)	89.8	7.0
	TMP (1)	90.3	3.5
HDmPyOC (**18b**)	DIEA (2)	92.0	20.7
	TMP (2)	88.0	7.9
HMPyOC (**18d**)	DIEA (2)	92.3	26.3
	TMP (2)	91.0	10.2
HTODC (**18e**)	TMP (2)	89.1	17.7
	TMP (1)[b]	82.3	16.3
HDMODC (**18g**)	DIEA (2)	88.0	17.9
	TMP (1)[b]	90.0	13.2
HDmPyODC (**18f**)	TMP (2)	87.2	22.1
HMPyODC (**18h**)	TMP (2)	89.4	23.2
HTOPC (**18k**)	TMP (2)	88.3	43.1
	TMP (1)	79.8	40.7
HDMOPC (**18l**)	TMP (2)	90.2	43.6
	TMP (1)	87.2	40.2

[a] LLL and LDL forms of the test tripeptide are described elsewhere.[7] Samples were co-injected with authentic and pure samples of LLL. HPLC system: linear gradient of 20% to 80% CH$_3$CN/0.1% TFA in H$_2$O/0.1%TFA over 30 min, detection at 200 nm, Waters C$_{18}$ 5 μm 4.6× 150 mm column, $t_{\text{R LLL}}$=19.98 min., $t_{\text{R LDL}}$=21.05 min. [b] Extra peak related to the starting material (Z-Phe-Val-OH) was observed in 3–5% ratio.

Table 7. Yields and racemization for the formation of Z-Phe-Val-Pro-NH$_2$ (2+1) in DMF (solid-phase synthesis).[a]

Coupling reagent	Base (equiv)	Yield [%]	LDL [%]
HATU (**4**)	TMP (2)	90.0	13.0
HBTU (**5**)	TMP (2)	89.0	27.0
HDMA (**7**)	TMP (2)	90.0	12.0
HDMB (**8**)	TMP (2)	92.0	23.0
6-HDMCB (**9**)	TMP (2)	92.0	20.0
HOTU (**18a**)	TMP (2)	91.0	27.1
	TMP (1)	85.0	25.0
COMU (**18c**)	TMP (2)	94.0	23.0
	TMP (1)	92.0	21.0
HTODC (**18e**)	TMP (2)	92.0	38.0
	TMP (1)	86.0	28.9
HDMODC (**18g**)	TMP (2)	94.0	25.7
	TMP (1)	88.0	23.3

[a] The coupling was performed with Fmoc-Pro-Rink amide-PS-resin and 3 equiv of Z-Phe-Val-OH, 3 equiv of coupling reagent, 6 equiv of base (TMP), and preactivation for 10–30 s in DMF at RT. The peptide was recovered after deblocking with water in TFA (10%) for 1 h at RT. The solvent was removed under vacuum and then washed with hexane. The crude peptide was injected into the HPLC system by using a previously reported method.[7] Extra peaks related to the starting material (Z-Phe-Val-OH) were observed in 3–5% percentages. LLL and LDL forms of the test tripeptide are described elsewhere.[7] Samples were co-injected with authentic and pure samples of LLL.

Fmoc-Aib-OH onto the Aib-containing resin were determined by reversed-phase HPLC analysis, after cleavage of the peptide from the resin (Table 8). The best results were obtained with the Oxyma-based COMU (**18c**) and HOTU (**18a**), with higher percentages of target pentapeptide being

Table 8. The percentages of des-Aib (H-Tyr-Aib-Phe-Leu-NH$_2$) obtained during solid-phase assembly of the pentapeptide (H-Tyr-Aib-Aib-Phe-Leu-NH$_2$).[a]

Coupling reagent	Base (equiv)	Pentapeptide [%]	des-Aib [%]
HATU (**4**)	DIEA (2)	83.0	17
	DIEA (1)	68.0	32
HBTU (**5**)	DIEA (2)	47.0	53
	DIEA (1)	33.0	67
HDMA (**7**)	DIEA (2)	98.0	<1
	DIEA (1)	90.0	10
HDMB (**8**)	DIEA (2)	89.0	10
	DIEA (1)	64.0	36
6-HDMCB (**9**)	DIEA (2)	98.7	1.3
	DIEA (1)	39.0	62.0
HOTU (**18a**)	DIEA (2)	99.0	1.0
	DIEA (1)[b]	0.3	99.7
	DIEA (2)[c]	87.5	12.5
COMU (**18c**)	DIEA (2)	99.7	0.26
	DIEA (1)[b]	29.3	70.7
	DIEA (2)[c]	99.86	0.14
HTODC (**18e**)	DIEA (2)	85.5	13.5
HDMODC (**18g**)	DIEA (2)	95.3	4.7
HTOPC (**18k**)	DIEA (2)	27.4	72.9
HDMOPC (**18 L**)	DIEA (2)	41.3	58.3

[a] Pentapeptide and deletion tetrapeptide des-Aib were confirmed by peak overlap in the presence of authentic samples. HPLC-MS showed the correct mass for the pentapeptide at 612.0. [b] 1 h standard single coupling was performed for Aib-Aib with only 1 equiv of base. [c] 30 min standard single coupling was performed for Aib-Aib with 2 equiv of base.

with the cyano-pyridinyl system (**18k**, **18l**) because of the higher acidity of the corresponding oxime.

For the same model but with the reaction carried out on solid-phase, COMU (**18c**) gave the best coupling yield, together with levels of racemization similar to those seen with the HOBt derivatives (Table 7).

To check the effectiveness of the new reagents, the demanding Leu-enkephalin derivative H-Tyr-Aib-Aib-Phe-Leu-NH$_2$[6f] was manually assembled on Fmoc-RinkAmide-AM-resin with the use of amino acid/activator (3 equiv), DIEA (6 or 3 equiv) and 30 min coupling times, except in the case of Aib-Aib, for which 1 h double coupling was used. Percentages of incorporation for the coupling of

These are not the final page numbers! ↗↗

obtained than with HDMA (**7**) or HATU (**4**). Synthesis with COMU (**18c**) led to only a 0.26 % yield of des-Aib when 2 equiv of DIEA were used, whereas its tetramethyl derivative **18a** gave a 1 % yield under the same conditions. For a 30 min coupling, **18c** gave a 0.14 % yield of des-Aib whereas **18a** gave a 12.5 % yield. This observation indicates that the morpholino moiety increases the reactivities of uronium salts relative to tetramethyl derivatives. These results are consistent with what is discussed above.

In view of the superiority showed by the morpholino-containing uronium salts over their tetramethyl counterparts, the effect of the leaving group was further tested by comparing the benzotriazole-based HDMA (**7**) and HDMB (**8**) and the Oxyma-based COMU (**18c**) in the manual solid-phase assembly of H-Tyr-MeLeu-MeLeu-Phe-Leu-NH$_2$ on Fmoc-RinkAmide-AM-PS-resin. The strategy followed for the assay began with the elongation of resin-bound tripeptide H-MeLeu-Phe-Leu-resin by use of DIC/Oxyma (**10**) in 30 min couplings. Quantitative yields were verified by means of the Kaiser test for primary amines. After this preliminary step, comparisons were made for the stepwise incorporation of the two last residues, with use of the corresponding immonium/uronium salt and Fmoc-amino acid. Samples were preactivated for 20–30 s with DIEA (2 or 1 equiv relative to uronium salt/Fmoc-amino acid) in order to avoid guanidylation of the growing peptide chain. The coupling times were shortened to 5 min, so that significant differences in the reactivities of the coupling reagents could arise. After cleavage from the resin with 90 % TFA/10 % H$_2$O and lyophilization, relative performances were checked in terms of percentages of pentapeptide and deletion peptides, as determined by reversed-phase HPLC analysis (Table 9).

The experiments were carried out either in standard (99.8 % purity, as determined by GC) or in treated (anhydrous, dried over molecular sieves and bubbled with N$_2$ to remove Et$_2$NH) DMF, as in the rest of experiments, in order to examine the effect of the solvent's purity (entries 1–6 vs. 7–12). The assay with standard DMF reflected the huge difference in reactivity between HOAt- and HOBt-derived uronium salts, with an impressive—for such demanding conditions—91 % yield of pentapeptide being obtained with HDMA (**7**), whereas HDMB (**8**) only afforded a poor 7 % (entries 1, 2). The Oxyma-based COMU (**18c**) gave a much higher purity than HDMB but, unlike in the previous synthesis of H-Tyr-Aib-Aib-Phe-Leu-NH$_2$, it was far from that afforded by HDMA (43 %, entry 3). The experiment was repeated, but with preactivation with only 1 equiv of base, a second equiv being added once the coupling mixture had been added onto the resin, in order to examine whether the base had any effect on the stability of the active ester during preactivation. The results showed no significant variation, except in the case of COMU (**18c**), for which the yield rose from 43 % to 55 % (due to the higher rate of coupling for the MeLeu residue), suggesting a high reactivity of the Oxyma-derived active ester (Table 9, entries 4, 5, and 6). The percentage of pentapeptide also increased to the same extent with COMU (**18c**) when the experiment with 2 equiv DIEA was carried out with treated, instead of standard, DMF, confirming the positive effect of the higher purity of the solvent, although this was not noticeable in the experiments with HDMA and HDMB (Table 9, entries 7, 8, and 9). Finally, an experiment was conducted with only 1 equiv DIEA, displaying the same tendency as observed previously: the performance of COMU (18c) was superior to that of the HOBt derivative but not as potent as that of the HOAt one (Table 9, entries 10, 11, and 12).

The effectiveness of COMU (**18c**) was compared with that of HOTU (**18a**) in the synthesis of the common decapeptide model ACP (65–74) on solid-phase (Table 10).[6f]

Table 10. Preparation of ACP (65–74) (H-Val-Gln-Ala-Ala-Ile-Asp-Tyr-Ile-Asn-Gly-NH$_2$) with use of the different coupling reagents (2 equiv) and 2 min coupling times.[a]

Coupling reagent	ACP [%]	Des-Asn [%]	Des-Val [%]	Des-Ile[69] [%]	Des-Ile[72] [%]
HOTU (**18a**)	66.0	0.27	2.72	21.7	7.56
COMU (**1cc**)	79.4	0.74	–	18.0	0.98

[a] The HPLC-MS showed the correct mass for the ACP at 1065.0.

The peptide was manually elongated on a Fmoc-Rink Amide-AM-resin (0.7 mmol g^{-1}). Coupling times of 2 min were used and excesses of reagents were 2 equiv for coupling reagents and amino acids and 4 equiv for DIEA. Incorporation was detected for Ile^{72} onto Asn and for Ile^{69} onto Asp. Peptide purity was determined by reversed-phase HPLC analysis, after cleavage of the peptide from the resin by treatment with TFA/H$_2$O (9:1) for 2 h at RT. HPLC analysis again showed a better performance of the morpholino-containing derivative than for the tetramethyl analogue: some deletion peptides, such as des-Val, were not observed with COMU (**18c**) and the percentage of pentapeptide ob-

Table 9. Percentages of H-Tyr-MeLeu-MeLeu-Phe-Leu-NH$_2$ and related deletion peptides obtained in solid-phase assembly in 5 min with use of various dimethyl-morpholino immonium/uronium salts.[a]

Entry	Coupling conditions		Coup. reagent	Penta [%]	des-MeLeu [%]	des-Tyr [%]	Trip [%]
1		2 equiv DIEA	HDMA	91.4	4.5	3.8	0.3
2			HDMB	7.0	42.2	9.7	41.1
3	standard DMF		COMU	42.9	48.5	4.4	4.2
4		2 equiv DIEA[b]	HDMA	91.5	5.0	3.1	0.4
5			HDMB	6.9	42.4	9.4	41.3
6			COMU	55.5	39.5	3.0	2.0
7		2 equiv DIEA	HDMA	89.4	6.7	3.6	0.3
8			HDMB	6.8	43.0	9.2	41.0
9	treated DMF		COMU	56.0	38.5	3.3	2.2
10		1 equiv DIEA	HDMA	73.7	18.5	7.4	0.4
11			HDMB	5.7	37.8	8.9	47.6
12			COMU	33.6	51.9	6.3	8.2

[a] HPLC-MS showed the correct mass for the pentapeptide at 695.5. Fmoc-amino acids were preactivated for 20–30 s. [b] Fmoc-amino acids were preactivated with only 1 equiv DIEA, with addition of another 1 equiv onto the resin after the first addition.

⤢⤢ These are not the final page numbers!

tained was higher than that obtained with HOTU (**18a**) (Table 10, entry 1 vs 2).

The safety profile of COMU (**18c**), the most efficient of the uronium salts tested, was also considered and compared to those of HDMA (**7**) and HDMB (**8**). This issue was highly relevant in view of the explosive properties of benzotriazole-based additives and derived stand-alone coupling reagents, which limit their transportation. Although explosivity has never been reported for HDMA (**7**) or HDMB (**8**), the fact that they contain HOBt/HOAt and that other immonium salts, such as TBTU, have also shown explosive properties[10] means that a certain safety risk is assumed. Our main interest was focused on checking whether the novel coupling reagent COMU (**18c**) would display the common pattern observed in explosive compounds: high release of pressure associated with rapid decomposition.[14]

The thermal risk was assessed through a combination of two calorimetry assays: Differential Scanning Calorimetry (DSC) and Accelerating Rate Calorimetry (ARC). A preliminary assessment of the risk associated with a given decomposition can be determined by means of a dynamic DSC experiment. The heat released during this assay is measured by comparing it with a reference that has undergone the same thermal process. In addition, the relative decomposition kinetics (which are linked to explosivity) are highlighted.[15] In this assay, samples are heated in a closed crucible under a flow of N_2 from 30 to 300 °C at a constant heating rate of 10 °C min^{-1}. Diagrams displaying the heat flow as a function of time and temperature showed a distinct difference in decomposition behavior between benzotriazole-based HDMA (**7**) and HDMB (**8**) and the novel COMU (Figure 7). During the decomposition of HDMA (**7**) and
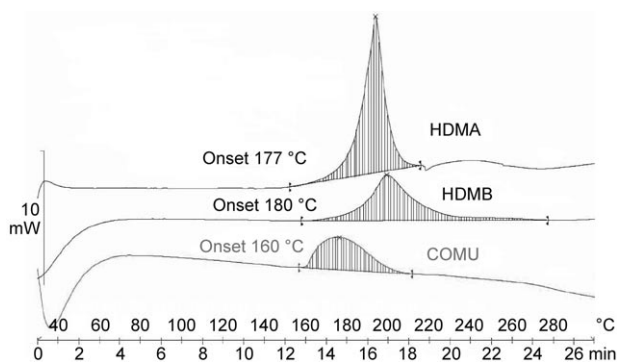
Figure 7. Thermograms showing heat flow versus temperature and time in the DSC experiments with HDMA (**7**), HDMB (**8**), and COMU (**18c**).

HDMB (**8**) the release of heat was slow at the beginning and increased very sharply, reaching a maximum and finally decreasing. This decomposition profile as observed for HDMA (**7**) and HDMB (**8**) resembles that of an autocatalytic reaction, in which the product also acts as a catalyst, the rate of the reaction increasing at the same time as the conversion.[16] These self-accelerating reactions warrant special attention because of their great unpredictability, result-

ing from the starting induction period with no thermal signal and their unexpected steep initiation. Therefore, a temperature alarm in an industrial process is not effective with compounds that show this kinetic behavior. Nevertheless, a dynamic DSC experiment can provide only indications of the autocatalytic nature of decomposition.

In contrast, COMU decomposed in a more constant manner that did not resemble this autocatalytic pattern. The normalized exothermic ΔH values should also be noted: 209 kJ mol^{-1} for HDMB, 245 kJ mol^{-1} for HDMA, and 183 kJ mol^{-1} for COMU. These observations indicate that in the event of an explosion, COMU would have less thermal severity. The ΔT_{ad} value (adiabatic temperature rise), calculated from experimentally ascertained exothermic ΔH values, also shows this relative severity: 248 °C for HDMB (**8**), 290 °C for HDMA (**7**), and 214 °C for COMU (**18c**). To conclude with the information that can be extracted from the DSC assay, the onset temperature at which decomposition began was lower in the case of the experiment with COMU (**18c**) (160 °C) than with HDMA (**7**) or HDMB (**8**) (177 °C and 180 °C, respectively).

A further evaluation of the risks associated with these compounds was carried out under adiabatic conditions by the ARC technique.[17] By this approach, the pressure released and the ΔT_{ad} can be directly determined. The assay begins with the application of the "heat-wait-seek" method, and when self-heating of the sample at a rate higher than 0.02 °C min^{-1} is detected, the experiment is changed to adiabatic mode. When decomposition occurs, the temperature and the pressure rise, and once the temperature reaches values above 300 °C the assay is stopped manually. In all cases the pressure rises detected were relatively low, in comparison with those of related additives.[11] In particular, the released pressure measured in the COMU (**18c**) experiment was similar to that seen with HDMA (**7**) (53 vs. 55 bar) and slightly higher than that seen with HDMB (**8**) (24 bar) (Figure 8).

Additionally, the increase in temperature during decomposition (ΔT_{ad}) was considerably lower with COMU (**18c**) (64 °C) than with HDMA (**7**) or HDMB (**8**) (164 °C and 121 °C, respectively), thereby confirming the lower thermal
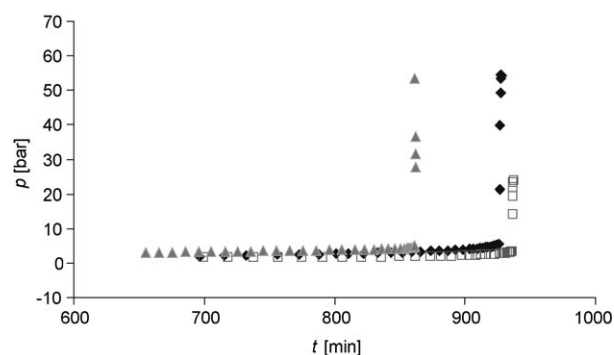

Figure 8. Decomposition profiles observed during ARC experiments with HDMB (**8**, □), HDMA (**7**, ◆), and COMU (**18c**, ▲) showing released pressure (bar) as a function of time (min).

These are not the final page numbers! ↗↗

severity of COMU observed in the DSC assay (Figure 9). Also consistent with the previous assay were the distinct kinetic profiles of COMU (**18c**) and the benzotriazole-based
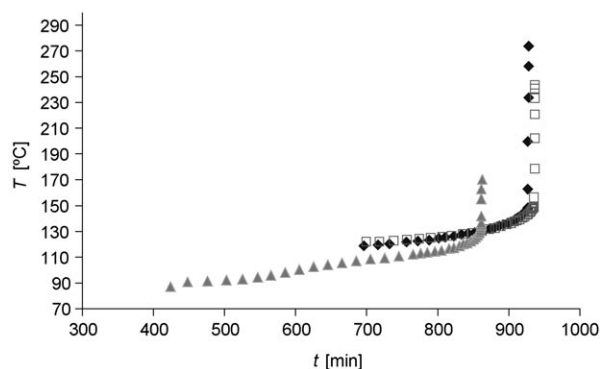

Figure 9. Decomposition profiles observed during ARC experiments with HDMB (**8**, □), HDMA (**7**, ♦), and COMU (**18c**, ▲) showing temperature (°C) as a function of time (min).

immonium salts. Whereas the temperatures in the HDMA (**7**) and HDMB (**8**) experiments increased slowly at the beginning and rose suddenly to their maxima (similarly to the DSC results, suggesting autocatylic kinetics), in the COMU (**18c**) experiment the temperature reached approximately one third of the total ΔT_{ad} over a period of time longer than had been required for the whole decomposition of HDMA (**7**) and HDMB (**8**). These slower kinetics could enable pressure originating from decomposition to be released into the environment.

With regard to the onset temperatures, ARC allows more accurate determination than DSC, which is known to suffer from uncertainty due to the smaller scale. For COMU (**18c**), decomposition began at a lower temperature than for HDMA (**7**) and HDMB(**8**) (91 °C vs. 119 °C and 122 °C). For safe working, it is recommended that the temperature of a given compound be maintained at values at which the time to maximum rate under adiabatic conditions is longer than 24 h.[18] This temperature can commonly be estimated after running an ARC assay, by subtraction of 50 K from the observed onset.[19] This safety value is at a lower temperature with COMU (**18c**) than with HDMA (**7**) and HDMB (**8**) (41 °C vs. 69 °C and 72 °C). Although peptide chemistry is usually performed at room temperature, and therefore below this safety threshold value, these results show that COMU has less thermal stability than benzotriazole-based immonium salts that also contain the morpholino moiety. The experimentally determined and calculated values determined from calorimetric studies and discussed above are shown in Table 11.

To study further the autocatalytic natures of the decompositions of HDMA (**7**) and HDMB (**8**), as suggested by the results obtained from the dynamic DSC and ARC experiments, in contrast with the results obtained for COMU (**18c**), we performed isothermal DSC assays. This technique is the most reliable way to detect whether decompositions

Table 11. Experimentally determined and calculated values obtained from dynamic DSC and ARC assays with the different stand-alone coupling reagents.

Coupling reagent	DSC			ARC		
	Onset [°C]	ΔH [kJ mol^{-1}]	calcd ΔT_{ad} [°C] [a]	Onset [°C]	Δp [bar]	exptl ΔT_{ad} [°C]
HDMA (**7**)	177	245	290	119	55	164
HDMB (**8**)	180	209	248	122	24	121
COMU (**18c**)	160	183	214	91	53	64

[a] Calculated ΔT_{ad} (°C) was obtained from the general formula ΔT_{ad} (°C) = ΔH (J mol^{-1})/[MW (g mol^{-1})·c_p (kJ kg^{-1} °C^{-1})], with estimated Cp = 2 kJ kg^{-1} °C^{-1}.

follow autocatalytic or non-autocatalytic kinetics. Temperatures were set at 10 °C below the onset observed in the corresponding dynamic DSC assay, and remained constant for 480 min. As a result, we obtained thermograms showing heat flow versus time (Figure 10). As would be expected for
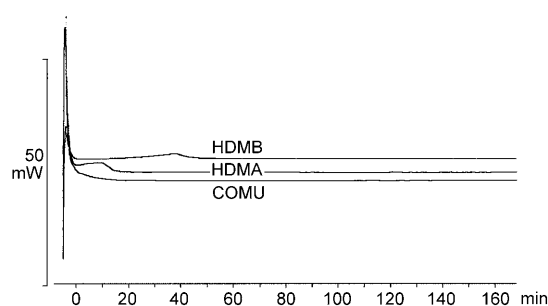

Figure 10. Thermograms showing heat flow versus time for isothermal DSC experiments set at 10 °C below the onset temperatures of HDMA (**7**, 167 °C), HDMB (**8**, 170 °C), and COMU (**18c**, 150 °C).

an autocatalytic reaction, HDMA (**7**) and HDMB (**8**) each defined a bell-shaped heat release curve, reported for this type of kinetics, in which the reaction accelerated, passing through a maximum of heat release and then decreasing. In contrast, COMU (**18c**) displayed a typical non-autocatalytic, nth-order kinetic profile, in which the rate of heat release decreased uniformly with time.[16] The former distinct kinetic profile strongly suggests the risk of a thermal runaway, which may lead to a sudden explosion, and consequently the safety measures that need to be taken.

Conclusions

In conclusion, we describe a new class of O-form uronium-type coupling reagents that differ in their immonium moieties and also in the leaving groups. The presence of the morpholino group has a marked influence on the polarity of the carbon skeleton, which affects the solubility, stability, and the reactivity of the reagent. As would be expected, HOAt derivatives were in all cases confirmed to be superior to HOBt ones in terms both of coupling yields and of retention

of configuration. Remarkably, Oxyma derivatives often gave results similar to or even better than those obtained with the aza derivatives, and also performed extremely well in the presence of only 1 equiv of base, thereby confirming the effect of the oxygen as a hydrogen bond acceptor in the reaction. The excellent performances of Oxyma derivatives, despite their acidities being similar to that of HOBt and higher than that of HOAt, can be explained by the fact that the *O*-form is the only form present during the coupling. In the benzotriazole derivatives, the *N*-form is the predominant one.

By means of calorimetry techniques, the safety profile of COMU (**18c**) was compared with those of benzotriazole-based HDMA (**7**) and HDMB (**8**). Although the pressure rises with the three coupling reagents were similar, COMU (**18c**) decomposed in a much slower and more controlled manner, with less thermal severity but greater predictability.[20] Moreover, the decomposition of HDMA (**7**) and HDMB (**8**), unlike that of COMU (**18c**), displayed autocatalytic kinetics, being highly unpredictable and difficult to detect before ending up in thermal runaway.

Experimental Section

General: TLC was performed on silica plates (8×4 cm, Albet) in suitable solvent systems with visualization with a Spectroline Model CM-10 UV lamp (254 nm). Melting points were measured in open capillary tubes with a Buchi B-540 melting point apparatus and were uncorrected. Infrared (IR) spectra were recorded on a Thermo Nicolet series Fourier Transformer instrument as KBr pellets. The absorption bands (ν_{max}) are given in wavenumbers (cm^{-1}). A Shimadzu UV-250/PC instrument was used as a UV/Vis spectrophotometer. NMR spectra were recorded on a Varian mercury 400 MHz spectrometer at room temperature. Tetramethylsilane (TMS) was used as reference for all NMR spectra, with chemical shifts reported as ppm relative to TMS. HPLC analyses were carried out with a Waters Symmetry Column C18, 5 μm, 4.6×150 mm with dual λ absorbance detector. HPLC-MS analyses were carried out with a Waters Symmetry Column C18, 5 μm, 4.6×150 mm with dual detector. All solvents used for recrystallization, extraction, column chromatography, and TLC were of commercial grade, distilled before use, and stored under dry conditions.

***N*,*N*-Dimethylmorpholine-4-carboxamide (DMU, 14a)**:[7] The urea derivative was distilled and collected at 127–129 °C as a colorless oil in a yield of 92.4 % (73 g from 0.5 mol reaction). ^{1}H NMR (CDCl$_3$): δ = 2.84 (s, 6H; 2CH$_3$), 3.22–3.2 (m, 4H; 2CH$_2$), 3.68–3.70 ppm (m, 4H; 2CH$_2$); ^{13}C NMR (CDCl$_3$): δ = 38.62, 47.51, 66.89, 164.96 ppm.

***N*,*N*-Dimethylpiperidine-1-carboxamide (DmPyU, 14b)**:[24,25] The pure urea was obtained as a colorless oil at 98–100 °C in a yield of 85.5 %. ^{1}H NMR (CDCl$_3$): δ = 1.81–2.10 (m, 4H; 2CH$_2$), 2.81 (s, 6H; 2CH$_3$), 3.15–3.18 ppm (m, 4H; 2CH$_2$).

Morpholino(pyrrolidin-1-yl)methanone (MPyU, 14c): The urea derivative was distilled and collected at 127–129 °C as a colorless oil in a yield of 92.4 % (73 g from 0.5 mol reaction). ^{1}H NMR (CDCl$_3$): δ = 2.84 (s, 6H; 2CH$_3$), 3.22–3.2 (m, 4H; 2CH$_2$), 3.68–3.70 ppm (m, 4H; 2CH$_2$); ^{13}C NMR (CDCl$_3$): δ = 38.62, 47.51, 66.89, 164.96 ppm.

General Procedure for the synthesis of chlorouronium salts:[26] Oxalyl chloride (100 mmol) in CH$_2$Cl$_2$ (100 mL) was added dropwise at room temperature over 5 min to a solution of urea derivative (100 mmol) in dry CH$_2$Cl$_2$ (200 mL). The reaction mixture was stirred under reflux for 3 h, and the solvent was removed under vacuum. The residue was washed with anhydrous ether (2×100 mL) and was then bubbled with N$_2$ to remove the excess of the ether. The obtained residue was very hygro-

scopic, so it was dissolved directly in CH$_2$Cl$_2$, and saturated aqueous potassium hexafluorophosphate (100 mmol in 50 mL water, KPF$_6$) was added at room temperature with vigorous stirring for 10–15 min. The organic layer was collected, washed once with water (100 mL), dried over anhydrous MgSO$_4$, and filtered. The solvent was removed under reduced pressure to give a white solid that was recrystallized from CH$_2$Cl$_2$/ether or acetonitrile/ether to give white crystals.

4-[(Dimethylamino)chloromethylene]morpholin-4-iminium hexafluorophosphate (DMCH, 15a):[7] The salt was obtained as white crystals in a yield of 89.6 % (28.9 g). M.p. 94– 95 °C; ^{1}H NMR (CD$_3$COCD$_3$): δ = 3.39 (s, 6H; 2CH$_3$), 3.75 (t, 4H; 2CH$_2$), 3.86 ppm (t, 4H; 2CH$_2$); ^{13} C NMR (CD$_3$COCD$_3$): δ = 44.36, 52.82, 65.99, 162.79 ppm.

***N*-[Chloro(pyrrolidin-1-yl)methylene]-*N*-methylmethanaminium hexafluorophosphate (DmPyCH, 15b)**:[23] The product was obtained as a white solid in a yield of 89.0 %. M.p. 93–95 °C; ^{1}H NMR (CD$_3$COCD$_3$): δ = 2.00–2.13 (m, 4H; 2CH$_2$), 3.49 (s, 6H; 2CH$_3$), 3.90–4.02 ppm (m, 4H; 2CH$_2$).

1-[Chloro(morpholino)methylene]pyrrolidinium hexafluorophosphate (MPyCH, 15c): The chloro salt was obtained by the method described above. The product was obtained as a white solid in a yield of 83.9 %. M.p. 99–100 °C; ^{1}H NMR ([D$_6$]acetone): δ = 2.10–2.14 (m, 4H; 2CH$_2$), 3.87 (t, 4H; 2CH$_2$), 4.00 (t, 4H; 2CH$_2$), 4.04–4.06 ppm (m, 4H; 2CH$_2$); ^{13}C NMR (CDCl$_3$): δ = 25.80, 51.75, 55.97, 65.97, 154.85 ppm; elemental analysis (%) calculated for C$_9$H$_{16}$ClF$_6$N$_2$OP (348.65): C 31.00, H 32.69, N 8.03; found: C 31.00, H 32.69, N 8.31.

General Procedure for preparation of uranium-type coupling reagents: The chloro salt (20 mmol) was added at 0 °C to a solution of an oxime potassium salt or a benzotriazole derivative (20 mmol) in acetonitrile (50 mL). The reaction mixture was stirred at this temperature for 30 min and was then allowed to come to room temperature with stirring over 6 h. The crude product was filtered and washed with acetonitrile. The solvent was concentrated to a small volume (1/4) under reduced pressure, and dry ether was then added to afford the product as a white solid in a pure state.

Synthesis of the potassium salt of hydroxycarbonimidoyl dicyanide (17a):[21] Sodium nitrite (14.2 g, 206 mmol) was slowly added at 0 °C (20–30 min addition) to a solution of malononitrile (9.06 g, 138 mmol) in acetic acid (20 mL) and water (50 mL). This mixture was then stirred at the same temperature for 45 min. After quenching of the reaction with HCl (2 N, 100 mL), the compound was extracted three times with ether (3×100 mL). The extracts were dried over anhydrous Na$_2$SO$_4$, and the ether was removed under vacuum to give an oily residue. The oily product was added slowly to a cold solution of KOH (8.0 g) in MeOH (100 mL), and then the reaction mixture was stirred for 20 min. Excess ether was added to afford the potassium salt as yellow crystals in a yield of 14.1 g (77.5 %). ^{13}C NMR (DMSO): δ = 107,40, 113.57, 119.78 ppm.

Synthesis of the potassium salt of diethyl 2-(hydroxyimino)malonate (17c):[22] A solution of diethyl malonate (16 g, 0.1 mol) in glacial acetic acid (17.5 mL, 0.3 mol) was stirred vigorously at 0–5 °C while a solution of NaNO$_2$ (20.7 g, 0.3 mol) in water (250 mL) was added dropwise over 3–4 h. The ice bath was removed and the mixture was stirred vigorously for a further 20 h. The nitrosation was carried out in three-necked flasks with appropriate fittings and a small vent to allow nitric oxide to escape. The reaction mixture was extracted with CH$_2$Cl$_2$ (400 mL and then 3× 100 mL portions). The combined CH$_2$Cl$_2$ extracts were dried over anhydrous Na$_2$SO$_4$. The CH$_2$Cl$_2$ was removed under vacuum and the resulting oily product was dissolved in CH$_2$Cl$_2$ (400 mL) and then stirred with anhydrous K$_2$CO$_3$ (32 g) for 15 min. After filtration, the CH$_2$Cl$_2$ was removed until 200 mL was reached, ether was added until the solution became cloudy, and the mixture was then kept in the refrigerator overnight to afford off-white crystals in 63.4 % yield. M.p. 116–118 °C; ^{1}H NMR (CDCl$_3$): δ = 1.24–1.29 (q, 6H; 2CH$_3$), 4.20–4.29 ppm (m, 4H; 2CH$_2$).

Synthesis of 2-pyridylhydroxyiminoacetonitrile (17d):[23] A solution of sodium nitrite (4.5 g, 0.065 mol in 5 mL water) was added slowly, with cooling, to a solution of 2-pyridylacetonitrile (2.2 g, 0.019 mol) in glacial acetic acid (4.5 mL). After 12 h standing, the precipitate was filtered off, washed with water, dried, and then recrystallized from ethanol to afford

These are not the final page numbers! ↗↗

the product in 65 % yield. M.p. 220–222 °C (lit. mp. 219–222 °C, 68 %); ^{1}H NMR ([D$_6$]DMSO: $\delta = 7.45$–7.52 (1 H), 7.87–7.90 (2 H), 8.67 (d, 1 H), 14.12 ppm (OH).

General Procedure for the preparation of urea derivatives:[24] The N,N-dialkylcarbamoyl chloride (0.6 mol) was added dropwise at 0 °C to a stirring mixture of secondary amine (0.5 mol) and triethylamine (TEA, 0.5 mol) in CH$_2$Cl$_2$ (400 mL). When the addition was complete, the mixture was stirred for 3–4 h at room temperature. The reaction mixture was basified with NaOH (10 %), and the organic layer was then collected and the aqueous layer was washed with CH$_2$Cl$_2$ (100 mL). The combined CH$_2$Cl$_2$ solution was washed with H$_2$O (2 × 100 mL) and saturated solution of NaCl (2 × 100 mL). Finally, the organic solvent was dried over anhydrous MgSO$_4$ and filtered, and the solvent was removed under reduced pressure. The oily residue obtained was purified by vacuum distillation.

***O*-[Cyano(ethoxycarbonyl)methylidene)amino]-1,1,3,3-tetramethyluronium hexafluorophosphate (HOTU, 18a)**: The product was obtained as a white solid in a yield of 6.32 g (82.1 %). M.p. 135–137 °C (dec). The triethylamine/HOXt approach gave a lower yield (68.7 %) than the potassium salt strategy, maybe due to the washing with water. ^{1}H NMR ([D$_6$]acetone): $\delta = 1.37$ (1, 3 H; CH$_3$), 3.37 (s, 12 H; 4 CH$_3$), 4.82 ppm (q, 2 H; CH$_2$); ^{13}C NMR ([D$_6$]acetone): $\delta = 13.46$, 40.71, 64.56, 106.78, 135.09, 156.11, 161.43 ppm; elemental analysis (%) calculated for C$_{10}$H$_{17}$F$_6$N$_4$O$_3$P (386.23): C 31.10, H 4.44, N 14.51; found: C 31.34, H 4.35, N 14.75.

1-[(1-(Cyano-2-ethoxy-2-oxoethylideneaminooxy)-dimethylamino-pyrrolidinomethylene)]methanaminium hexafluorophosphate (HDmPyOC, 18b): The product was obtained as a white solid, in a yield of 6.8 g (82.7 %). M.p. 126–127 °C (dec); ^{1}HNMR ([D$_6$]acetone): $\delta = 1.37$ (t, 3 H; CH$_3$), 2.10, 2.13 (m, 4 H; 2 CH$_2$), 3.36 (s, 6 H; 2 CH$_3$), 3.95–3.99(m, 4 H; 2 CH$_2$), 4.48 ppm (q, 2 H; CH$_2$); ^{13}C NMR ([D$_6$]acetone): $\delta = 13.47$, 25.09, 40.40, 51.58, 64.52, 106.74, 134.82, 156.12, 158.66 ppm; elemental analysis (%) calculated for C$_{12}$H$_{19}$F$_6$N$_4$O$_3$P (412.27): C 34.96, H 4.65, N 13.59; found: C 35.07, H 4.79, N 13.72.

1-[(1-(Cyano-2-ethoxy-2-oxoethylideneaminooxy)-dimethylamino-morpholinomethylene)]methanaminium hexafluorophosphate (COMU, 18c): The product was obtained as white crystals in a yield of 7.6 g (88.8 %), and decomposes without melting at 159.90 °C according to dynamic DSC (Figure 3). ^{1}H NMR ([D$_6$]acetone): $\delta = 1.38$ (t, 3 H; CH$_3$), 3.41 (s, 6 H; 2 CH$_3$), 3.82 (t, 4 H; 2 CH$_2$), 3.89 (t, 4 H; 2 CH$_2$), 4.48 ppm (q, 2 H; CH$_2$); ^{13}C NMR ([D$_6$]acetone): $\delta = 13.48$, 40.70, 49.94, 64.59, 66.04, 106.76, 135.03, 156.14, 160.61 ppm; elemental analysis (%) calcd for C$_{12}$H$_{19}$F$_6$N$_4$O$_4$P (428.27): C 33.65, H 4.47, N 13.08; found: C 33.79, H 4.59, N 13.30.

1-[(1-Cyano-2-ethoxy-2-oxoethylideneaminooxy)(morpholino)methylene]pyrrolidinium hexafluorophosphate (HMPyOC, 18d): The product was obtained as white solid in a yield of 8.2 g (90.3 %). M.p. 171–172 °C; ^{1}H NMR ([D$_6$]acetone): $\delta = 1.26$ (t, 3 H; CH$_3$), 1.98–2.02 (m, 4 H; 2 CH$_2$), 3.65–3.68 (m, 4 H; 2 CH$_2$), 3.74–3.76 (m, 4 H; 2 CH$_2$), 3.84–3.87 (m, 4 H; 2 CH$_2$), 4.37–4.40 ppm (q, 2 H; CH$_2$); ^{13}C NMR ([D$_6$]acetone): $\delta = 13.49$, 25.09, 49.20, 51.57, 55.98, 51.76, 64.54, 66.06, 106.69, 134.63, 156.11, 157.88 ppm; elemental analysis (%) calcd for C$_{14}$H$_{21}$F$_6$N$_4$O$_4$P (454.31): C 37.01, H 4.66, N 12.33; found: C 37.25, H 4.78, N 12.50.

***O*-[(Dicyanomethylidene)amino]-1,1,3,3-tetramethyluronium hexafluorophosphate (HTODC, 18e)**: The product was obtained as a white solid in a yield of 5.0 g (74.0 %). M.p. 180–181 °C (dec); ^{1}H NMR ([D$_6$]acetone): $\delta = 3.27$ (s, 12 H; 4 CH$_3$) ppm; ^{13}C NMR ([D$_6$]acetone): $\delta = 40.80$, 105.10, 108.21, 119.65, 160.67 ppm; elemental analysis (%) calcd for C$_8$H$_{12}$F$_6$N$_5$OP (339.18): C 28.33, H 3.57, N 20.65; found: C 28.52, H 3.65, N 20.88.

1-{[1-(Dicyanomethylideneaminooxy)-dimethylamino-pyrrolodinomethylene]}methanaminium hexafluorophosphate (HDmPyODC, 18f): The product was obtained as a light yellow solid, in a yield of 5.4 g (74 %). M.p. 146–147 °C (dec). ^{1}H NMR ([D$_6$]acetone): $\delta = 1.97$–2.00 (m, 4 H; 2 CH$_2$), 3.28 (s, 6 H; 2 CH$_3$), 3.96–4.04 (m, 4 H; 2 CH$_2$) ppm. ^{13}C NMR ([D$_6$]acetone): $\delta = 25.07$, 40.41, 51.77, 105.06, 108.23, 119.30, 157.86 ppm; elemental analysis (%) calculated for C$_{10}$H$_{14}$F$_6$N$_5$OP (365.22): C 32.89, H 3.86, N 19.18; found: C 33.12, H 3.99, N 19.51.

1-{[1-(Dicyanomethyleneaminooxy)-dimethylamino-morpholinomethylene)]methanaminium hexafluorophosphate (HDMODC, 18g): The product was obtained as white solid in a yield of 5.7 g (74.8 %). M.p. 118–119 °C; ^{1}H NMR ([D$_6$]acetone): $\delta = 3.42$ (s, 6 H; 2 CH$_3$), 3.80–3.88 ppm (m, 8 H; 4 CH$_2$); ^{13}C NMR ([D$_6$]acetone): $\delta = 40.97$, 49.93, 65.92, 105.13, 108.15, 119.84, 159.77 ppm; elemental analysis (%) calcd for C$_{10}$H$_{14}$F$_6$N$_5$O$_2$P (381.21): C 31.51, H 3.70, N 18.37; found: C 31.68, H 3.84, N 18.61.

1-[(Dicyanomethyleneaminooxy)(morpholino)methylene]pyrrolidinium hexafluorophosphate (HMPyODC, 18h): The product was obtained as light yellow solid in a yield of 6.4 g (78.6 %). M.p. 158–159 °C; ^{1}H NMR ([D$_6$]acetone): $\delta = 2.11$–2.14 (m, 4 H; 2 CH$_2$), 3.79–3.85 (m, 4 H; 2 CH$_2$), 3.86–3.88 (m, 4 H; 2 CH$_2$), 3.98–4.01 ppm (m, 4 H; 2 CH$_2$); ^{13}C NMR ([D$_6$]acetone): $\delta = 25.28$, 49.15, 65.95, 105.07, 108.17, 119.48, 157.00 ppm; elemental analysis (%) calcd for C$_{12}$H$_{16}$F$_6$N$_5$O$_2$P (407.25): C 35.39, H 3.96, N 17.20; found: C 35.60, H 4.06, N 17.56.

***O*-[(Diethoxycarbonylmethylidene)amino]-1,1,3,3-tetramethyluronium hexafluorophosphate (HTODeC, 18i)**: The product was obtained as a pale yellow oil in a yield of 84.5 %. ^{1}H NMR (CDCl$_3$): $\delta = 1.35$ (t, 6 H; 2 CH$_3$), 3.18 (s, 12 H; 4 CH$_3$), 4.39–4.48 ppm (q, 4 H; 2 CH$_2$); elemental analysis (%) calcd for C$_{12}$H$_{22}$F$_6$N$_3$O$_5$P (433.28): C 33.26, H 5.12, N 9.70; found: C 33.44, H 5.25, N 9.98.

1-[(1,3-Diethoxy-1,3-dioxoprop-2-ylideneaminooxy)-dimethylamino-morpholinomethylene)]methanaminium hexafluorophosphate (HDMODeC, 18j): The product was obtained as pale yellow oil in a yield of 84.3 %. ^{1}H NMR (CDCl$_3$): $\delta = 1.35$ (t, 6 H; 2 CH$_3$), 3.21(s, 6 H; 2 CH$_3$), 3.35 (t, 2 H; CH$_2$), 3.61 (t, 2 H; CH$_2$), 3.78 (t, 2 H; CH$_2$), 3.87 (t, 2 H; CH$_2$), 4.37–4.50 ppm (q, 4 H; 2 CH$_2$); elemental analysis (%) calcd for C$_{14}$H$_{24}$F$_6$N$_3$O$_6$P (475.32): C 35.38, H 5.09, N 8.84; found: C 35.53, H 5.28, N 9.11.

***N*-{[Cyano(pyridin-2-yl)methyleneaminooxy](dimethylamino)methylene}-*N*-methylmethanaminium hexafluorophosphate (HTOPC, 18k)**: The product was obtained as a light reddish brown solid in a yield of 6.2 g (82.7 %). M.p. 169–171 °C; ^{1}H NMR ([D$_6$]acetone): $\delta = 3.30$ (s, 12 H; 4 CH$_3$), 7.57–7.61 (m, 1 H), 7.94 (td, 1 H), 8.10 (dd, 1 H), 8.70 ppm (dd, 1 H); ^{13}C NMR ([D$_6$]acetone): $\delta = 40.48$, 107.56, 122.52, 127.87, 138.18, 142.46, 146.67, 150.68, 162.03 ppm; elemental analysis (%) calcd for C$_{12}$H$_{16}$F$_6$N$_5$OP (391.25): C 36.84, H 4.12, N 17.90; found: C 37.00, H 4.21, N 18.11.

***N*-{[Cyano(pyridin-2-yl)methyleneaminooxy](dimethylamino)methylene}-*N*-morpholinomethanaminium hexafluorophosphate (HDMOPC, 18l)**: The product was obtained as a light brown solid in a yield of 7.74 g (89.4 %). M.p. 154–155 °C; ^{1}H NMR ([D$_6$]acetone): $\delta = 3.34$ (s, 12 H; 4 CH$_3$), 3.79–3.83 (m, 8 H; 4 CH$_2$), 7.58–7.62 (m, 1 H), 7.96 (td, 1 H), 8.12 (dd, 1 H), 8.71 ppm (dd, 1 H); ^{13}C NMR ([D$_6$]acetone): $\delta = 40.76$, 49.79, 66.13, 107.60, 122.53, 127.92, 138.23, 142.74, 146.63, 150.69, 161.06 ppm; elemental analysis (%) calcd for C$_{14}$H$_{18}$F$_6$N$_5$O$_2$P (433.29): C 38.81, H 4.19, N 16.16; found: C 39.04, H 4.33, N 16.47.

1-[Morpholino(pyrrolidinium-1-ylidene)methyl]-1*H*-[1.2.3]triazolo[4,5-I]pyridine 3-oxide hexafluorophosphate (HMPyA, 19): The product was obtained as a white solid in a yield of 7.3 g (81.3 %). M.p. 206–208 °C (dec); ^{1}H NMR ([D$_6$]acetone): $\delta = 2.11$–2.15 (m, 2 H; CH$_2$), 2.18–2.30 (m, 2 H; CH$_2$), 3.48–3.63 (m, 2 H; CH$_2$), 3.79–4.16 (m, 10 H; 5 CH$_2$), 8.02 (dd, 1 H), 8.53 (dd, 1 H), 8.85 ppm (dd, 1 H); ^{13}C NMR ([D$_6$]acetone): $\delta = 25.09$, 41.74, 42.35, 50.82, 51.58, 66.19, 66.42, 124.37, 127.84, 149.65 ppm; elemental analysis (%) calcd for C$_{14}$H$_{19}$F$_6$N$_6$O$_2$P (448.30): C 37.51, H 4.27, N 18.75; found: C 37.75, H 4.42, N 19.02.

1-[Morpholino(pyrrolidinium-1-ylidene)methyl]-1*H*-benzo[*d*]-[1.2.3]triazole 3-oxide hexafluorophosphate (HMPyB, 20): The product was obtained as a white solid in a yield of 7.4 g (82.8 %). M.p. 203–204 °C (dec); ^{1}H NMR ([D$_6$]acetone): $\delta = 2.12$–2.15 (m, 2 H; CH$_2$), 2.16–2.29 (m, 2 H; CH$_2$), 3.42–3.58 (m, 2 H; CH$_2$), 3.80–4.26 (m, 10 H; 5 CH$_2$), 7.75 (td, 1 H), 7.97–8.02 (m, 2 H), 8.07 ppm (d, 1 H); ^{13}C NMR ([D$_6$]acetone): $\delta = 25.09$, 41.76, 42.23, 50.81, 51.51, 66.19, 66.41, 109.99, 114.56, 127.52, 143.54 ppm. elemental analysis (%) calcd for C$_{15}$H$_{20}$F$_6$N$_5$O$_2$P (447.32): C 40.28, H 4.51, N 15.66; found: C 40.45, H 4.66, N 15.89.

5-Chloro-1-[morpholino(pyrrolidinium-1-ylidene)methyl]-1H-benzo[d]-[1.2.3]triazole 3-oxide hexafluorophosphate (HMPyC, 21): The product was obtained as a white solid in a yield of 7.96 g (82.7%). M.p. 217–218°C (dec); ^{1}H NMR ([D$_6$]acetone): δ = 2.10–2.15 (m, 2H; CH$_2$), 2.19–2.29 (m, 2H; CH$_2$), 3.45–3.65 (m, 2H; CH$_2$), 3.81–4.09 (m, 10H; 5CH$_2$), 7.99 (d, 1H), 8.02 (d, 1H), 8.12 ppm (dd, 1H); ^{13}C NMR ([D$_6$]acetone): δ = 25.93, 52.89, 53.36, 66.09, 66.42, 115.79, 115.84, 132.57, 132.62, 134.06, 134.12, 147.38 ppm; elemental analysis (%) calculated for C$_{15}$H$_{19}$ClF$_6$N$_5$O$_2$P (481.76): C 37.40, H 3.98, N 14.54; found: C 37.65, H 4.13, N 14.79.

Fmoc-Val-Val-NH$_2$ in solution phase: An authentic sample was prepared as follows: Tetramethylfluoroformamidiniun hexafluorophosphate (TFFH, 1 mmol) was added at 0°C to a mixture of Fmoc-Val-OH (1 mmol), and DIEA (1 mmol) in DMF (5 mL) and the reaction mixture was activated for 5 min, followed by the addition of H-Val-NH$_2$ (1 mmol) and DIEA (1 mmol). The reaction mixture was stirred at 0°C for 1 h and at RT for 3 h. Water (50 mL) was added and the precipitate was collected and washed with sat. Na$_2$CO$_3$ and HCl (1 N), and was then dried in air and recrystallized from ethyl acetate/hexane to give a white solid in a yield of 87.0%. M.p. 226–228°C. ^{1}H NMR ([D$_6$]DMSO): δ = 0.95 (t, 12H; 4CH$_3$), 1.80–2.00 (m, 2H; 2CH), 3.87 (t, 1H; CH), 4.10 (t, 1H; CH), 4.18–4.20 (m, 3H; CH, CH$_2$), 7.02 (t, 2H; NH), 7.28–7.85 ppm (m, 12, ar, NH).

This sample was used as an authentic sample and injected into the HPLC (Waters 2487) under the following conditions: linear gradient of 10 to 90% CH$_3$CN/0.1% TFA in H$_2$O/0.1% TFA over 30 min, detection at 200 nm. Flow rate = 1 mL min^{-1}. Column: Waters C$_{18}$, 5 μm, 4.6×150mm (Waters Dual Wavelength Detector and Waters 717 Plus auto sampler). t_R = 20.89 min (Fmoc-Val-OH), t_R = 19.88 min (Fmoc-Val-Val-NH$_2$). This reaction was repeated under several sets of coupling conditions and samples (10 μL) were taken at different intervals. In addition, the reaction was quenched by addition of acetonitrile/water (1:1, 2 mL), and a sample of the solution (10 μL) was then injected into the HPLC system under the same conditions as described above.

Z-Aib-Val-OMe in solution phase: An authentic sample was prepared as follows: TFFH (0.264 g, 1 mmol) was added at 0°C to a mixture of Z-Aib-OH (0.237 g, 1 mmol), and DIEA (0.174 mL, 1 mmol) in DMF (5 mL) and the reaction mixture was activated for 8 min, followed by addition of H-ValO-Me·HCl (0.169 g, 1 mmol) and DIEA (2 mmol). The reaction mixture was stirred at 0°C for 1 h and at RT for 3 h. Water (50 mL) was added, and the precipitate was collected and washed with sat. Na$_2$CO$_3$ and HCl (1 N), and was then dried in air and recrystallized from dichloromethane/hexane (white needles after two days at room temperature) to give a white solid in 87.0% yield. M.p. 76–77°C; ^{1}H NMR ([D$_6$]DMSO): δ = 0.85 (t, 6H; 2CH$_3$), 1.56 (d, 6H; 2CH$_3$), 2.13–2.18 (m, 1H; CH), 3.72 (s, 3H; OCH$_3$), 4.49–4.53 (m, 1H; CH), 5.09 (s, 2H; CH$_2$), 5.36 (br s, 1H; NH), 7.28–7.37 (m, 6H; ar, NH) ppm. This sample was used as an authentic sample and injected into the HPLC (Waters 2487) under the following conditions: linear gradient of 10 to 90% CH$_3$CN/0.1% TFA in H$_2$O/0.1%TFA over 30 min, detection at 200 nm. Flow rate = 1 mL min^{-1}. Column: Waters C$_{18}$, 5 μm, 4.6×150mm. (Waters Dual Wavelength Detector and Waters 717 Plus auto sampler). t_R (Z-Aib-OH) = 18.25 min, t_R (Z-Aib-Val-OMe) = 20.90 min, t_R (Z-Aib-OAt) = 22.30 min, t_R (Z-Aib-OBt) = 22.80 min, t_R (Z-Aib-Oxyma) = 23.90 min.

Model segment coupling reaction: Test couplings were carried out as previously described for Z-Phg-Pro-NH$_2$[7] and Z-Phe-Val-Pro-NH$_2$.[7]

Synthesis of Tyr-Aib-Aib-Phe-Leu-NH$_2$ on solid phase:[6d] Fmoc-Rink Amide-PS (100 mg, 0.7 mmol g^{-1}) was deblocked with piperidine in DMF (20%, 10 mL) for 10 min and washed with DMF (2×10 mL), CH$_2$Cl$_2$ (2× 10 mL), and then DMF (2×10 mL). Fmoc-Leu-OH (3 equiv), coupling reagent (3 equiv), and DIEA (6 equiv) were mixed in DMF (0.5 mL) for activation (1–2 min) and then added to the resin. The reaction mixture was then stirred slowly for 1 min and allowed to couple for 30 min (1 h, double coupling only for the Aib-Aib). The resin was washed with DMF, and then deblocked with piperidine in DMF (20%) for 7 min. It was then again washed with DMF, CH$_2$Cl$_2$, and DMF and coupled with the next amino acid. Coupling and deblocking steps were repeated to provide

the pentapeptide. The crude product was analyzed by HPLC with a linear gradient of 20 to 80% CH$_3$CN/0.1% TFA in H$_2$O/0.1% TFA over 30 min on a Symmetry Waters C$_{18}$ column (4.6×150mm, 4 μm), with detection at 220 nm, flow rate 1.0 mL min^{-1}, t_R (penta) = 8.82 min, t_R (des-Aib) = 9.10 min.

Synthesis of H-Tyr-MeLeu-MeLeu-Phe-Leu-NH$_2$ on solid phase: Tripeptide H-MeLeu-Phe-Leu-NH$_2$ was manually assembled on Fmoc-RinkA-mide-Aminomethyl-PS-resin (0.63 mmol g^{-1}), after Fmoc removal with piperidine in DMF (20%, 2×5 min). The resin was washed with DMF (×10), CH$_2$Cl$_2$ (×10), and DMF (×10). Residues were introduced after 30 min coupling, with preactivation of Fmoc-amino acids (3 equiv) with Oxyma (3 equiv) and DIC (3 equiv) in DMF for 1.5 min. Quantitative incorporation was checked at each step by use of the Kaiser test for primary amines. Sample cleavage (10 mg) with TFA/H$_2$O (9:1) confirmed the tripeptide in >99.5% purity, as analyzed by reversed-phase HPLC and ESI-MS ([M+H]$^+$ = 405.32). The two last residues, Tyr and MeLeu, were introduced by preparation of 0.3 M solutions of coupling reagent (3 equiv) and Fmoc-amino acid (3 equiv) in standard or treated DMF, and preactivation of the mixture with DIEA (3 or 6 equiv) for 20–30 s. The peptide chain was cleaved from the resin with TFA/H$_2$O (9:1) over 2 h at room temperature. The solution was filtered and the resin was washed with CH$_2$Cl$_2$ (1 mL×2), which was removed together with TFA under nitrogen flow. The crude peptide was purified with cold Et$_2$O (2 mL×3) and after lyophilization, purity was checked on reversed-phase HPLC, with use of a Waters SunFire C18 Column (3.5 μm, 4.6×100mm), with a 20% to 50% linear gradient of 0.036% TFA in CH$_3$CN/0.045% TFA in H$_2$O over 8 min, with detection at 220 nm. The t_R of the pentapeptide was 6.5 min, whereas the t_R values of des-MeLeu, des-Tyr, and tripeptide H-MeLeu-Phe-Leu-NH$_2$ were 5.0, 5.7, and 3.0 min respectively.

Synthesis of ACP (65–74) (H-Val-Gln-Ala-Ala-Ile-Asp-Tyr-Ile-Asn-Gly-NH$_2$):[6d] The peptide was elongated manually on an Fmoc-Rink Amide-AM-resin (0.7 mmol g^{-1}). Coupling times of 2 min were used, and excesses of reagents were 2 equiv for Fmoc-amino acids and coupling reagents and 4 equiv for DIEA. Incorporation was detected for Ile^{72} onto Asn and for Ile^{69} onto Asp. Peptide purity was determined by reversed-phase HPLC analysis (Symmetry Waters C$_{18}$ (4.6×150mm, 4 μm), linear gradient over 30 min of 10 to 90% CH$_3$CN in H$_2$O/0.1% TFA, flow rate 1.0 mL min^{-1}, t_R decapeptide = 10.43 min, t_R des-Asn = 10.8 min, t_R des-Ile^{72} = 7.5 min, t_R des-Ile^{69} = 9.1 min, t_R des-Val = 8.43 min), after cleavage of the peptide from the resin by treatment with TFA/H$_2$O (9:1) for 2 h at room temperature.

General Procedure for dynamic differential scanning calorimetry assays: The thermal behavior of HDMA (**7b**), HDMB (**8**), and COMU (**18c**) was tested. Samples (1 mg) were heated from 30°C to 300°C at a rate of 10°C min^{-1} in a closed high-pressure crucible with N$_2$ flow in a Mettler–Toledo DSC-30 differential scanning calorimeter. Diagrams showing heat flow as a function of temperature and time were obtained.

General Procedure for isothermal differential scanning calorimetry assays: The autocatalytic natures of HDMA (**7b**), HDMB (**8**), and COMU (**18c**) was tested. Samples (1 mg) were heated to 10°C below the onset temperatures detected in the dynamic DSC [HDMA (**7**): 167°C, HDMB (**8**): 170°C, and COMU (**17c**): 150°C] for 480 min in a closed high-pressure crucible with N$_2$ flow in a Mettler–Toledo DSC-30 differential scanning calorimeter. Diagrams showing heat flow as a function of time were obtained.

General Procedure for ARC experiments: Assays were carried out on an Accelerating Rate Calorimeter (ARC) from Thermal Hazard Technology, with use of ARCTC-HC-MCQ (Hastelloy) test cells. Samples [1.837 g of HDMB (**8**), 1.605 of HDMA (**7**), and 2.350 g of COMU (**18c**)] were introduced into the calorimetric test cell at room temperature, without stirring. The cell was heated at the initial temperature (30°C) and the "heat-wait-seek" method was applied. This procedure consisted of heating the sample by 5°C and, after 15 min of equilibrium, measuring whether self-heating was occurring at a rate higher than 0.02°C min^{-1} (default sensitivity threshold). When self-heating was detected, the system was changed to adiabatic mode. After decomposition, the assay

was stopped when temperature rose above 300 °C. The phi factors[27] were: 2.02371 (HDMA), 2.76093 (HDMB), and 2.40644 (COMU).

Acknowledgements

[1] Abbreviations not defined in text: Aib, α-aminoisobutyric acid; DIEA, *N,N*-diisopropylethylamine; DMF, *N,N*-dimethylformamide; HOBt, 1-hydroxybenzotriazole; HOAt, 7-aza-1-hydroxybenzotriazole; N-HATU, N-[(dimethylamino)-1H-1,2,3-triazolo[4,5-b]pyridin-1-yl-methylene]-*N*-methylmethanaminium hexafluorophosphate N-oxide; N-HBTU, N-[(1H-benzotriazol-1-yl)-(dimethylamino)methylene]N-methylmethanaminium hexafluorophosphate N-oxide; DMCH,4-((dimethyamino)chloromethylene)morpholin-4-Iminium hexaflurophosphate HDMA, 1-((dimethylimino)morpholino > methyl)3-*H*-[1,2,3]triazolo[4,5-*b*]pyridine-1–3-olate hexafluorophosphate; HDMB, 1-((dimethylimino)morpholino > methyl)3-*H*-benzo-[1,2,3]triazolo-1-ium-3-olate hexafluorophosphate; 6-HDMCB, 1-((dimethylimino)morpholino > methyl)3-*H*-6-chlorobenzo[1,2,3] triazolo-1-ium-3-olate hexafluorophosphate; DMU, *N,N*-dimethylmorpholine-4-carboxamide; DmPyU, *N,N*-Dimethylpiperidine-1-carboxamide; MPyU, Morpholino(pyrrolidin-1-yl)methanone; *N*-DmPyCH, (Chloro(pyrrolidin-1-yl)methylene)-*N*-methylmethanaminium hexafluorophosphate; MPyCH, 1-(chloro(morpholino)methylene)pyrrolidinium Hexafluorophosphate; HOTU, O-[Cyano(ethoxycarbonyl)methylidene)amino]-1,1,3,3-tetramethyluronium Hexafluorophosphate; HdmPyOC, 1-[(1-(Cyano-2-ethoxy-2-oxoethylideneaminooxy)-dimethylamino-pyrrolodinomethylene)] methanaminium Hexafluorophosphate; COMU, 1-[(1-(Cyano-2-ethoxy-2-oxoethylideneaminooxy)-dimethylamino-morpholinomethylene)] methanaminium Hexafluorophosphate; HMPyOC, 1-((1-cyano-2-ethoxy-2-oxoethylideneaminooxy)(morpholino)methylene) pyrrolidinium Hexafluorophosphate; HTODC, O-[(Dicyanomethylidene)-amino]-1,1,3,3-tetramethyluronium Hexafluorophosphate; HDmPyODC, 1-[(1-(dicyanomethylideneaminoxy)-dimethylamino-pyrrolodinomethylene)] methanaminium Hexafluorophosphate; HDMODC, 1-[(1-(dicyanomethyleneaminooxy)-dimethylamino-morpholinomethylene)] methanaminium Hexafluorophosphate HMPyODC, 1-((dicyanomethyleneaminooxy)morpholinomethylene)pyrrolidinium Hexafluorophospoate; HTODeC, O-[(diethoxycarbonylmethylidene)amino]-1,1,3,3-tetramethyluronium Hexafluorophosphate; HDMODeC, 1-[(1,3-diethyoxy-1,3-dioxopropan-2-ylideneaminooxy)-dimethylamino-morpholinomethylene)] methanaminium Hexafluorophosphate; HTOPC, *N*-[(cyano(pyridine-2-yl)methyleneaminooxy)(dimethylamino)methylene)-*N*-Methylmethanaminium Hexafluorophosphate; HDMOPC, *N*-[(cyano(pyridine-2-yl)methyleneaminooxy)(dimethylamino)methylene)-*N*-morpholino-methanaminium Hexafluorophosphate; HMPyA, 1-(morpholino-(pyrrolidinium-1-ylidene)methyl)-*1H*-[1,2,3]triazolo[4,5-I]pyridine 3-oxide Hexafluorophosphahte; HMPyB, 1-(morpholino(pyrrolidinium-1-ylidene)methyl)-*1H*-benzo[*d*][1,2,3]triazole 3-oxide Hexafluorophosphate; HMPyC, 5-chloro-1-(morpholino(pyrrolidinium-1-ylidene)methyl)-*1H*-benzo[*d*][1,2,3]triazole 3-oxide hexafluorophosphate; Amino acids and peptides are abbreviated and designated following the rules of the IUPAC-IUB Commission of Biochemical Nomenclature [*J. Biol. Chem.* **247**, 977 (1972)].

[2] a) P. Lloyd-Williams, F. Albericio, E. Giralt, *Chemical Approaches to the Synthesis of Peptides and Proteins*, CRC, Boca Raton, **1997**; b) *Synthesis of Peptides and Peptidomimetics, Houben-Weyl, Methods of Organic Chemistry, Vol. E22a* (Ed.: M. Goodman), Thieme, Stuttgart, **2002**; c) M. Amblard, J.-A. Fehrentz, J. Martinez, G. Subra, *Mol. Biotechnol.* **2006**, *33*, 239–254.

[3] a) F. Albericio, L. A. Carpino in *Methods in Enzymology, Solid-Phase Peptide Synthesis, Vol. 289* (Ed.: G. B. Fields), Academic Press, Orlando, **1997**, pp. 104–126; b) J. M. Humphrey, A. R. Chamberlin, *Chem. Rev.* **1997**, *97*, 2243–2266; c) Z. J. Kaminski, *Biopolymers* **2000**, *55*, 140–165; d) F. Albericio, R. Chinchilla, D. J. Dodsworth, C. Najera, *Org. Prep. Proceed. Int.* **2001**, *33*, 203–303; e) S-Y. Han, Y-A. Kim, *Tetrahedron* **2004**, *60*, 2447–2467; f) C. A. G. N. Montalbetti, V. Falque, *Tetrahedron* **2005**, *61*, 10827–10852.

[4] V. Dourtoglou, J. C. Ziegler, B. Gross, *Tetrahedron Lett.* **1978**, 1269–1272.

[5] F. Albericio, J. M. Bofill, A. El-Faham, S. A. Kates, *J. Org. Chem.* **1998**, *63*, 9678–9683.

[6] a) P. Henklein, M. Beyermann, M. Bienert, R. Knorr, in *Proceedings of the 21st European Peptide Symposium* (Eds.: E. Giralt, D. Andreu), Escom Sience, Leiden, **1991**, pp. 67–68, b) R. Knorr, A. Trzeciak, W. Bannwarth, D. Gillessen in *Peptide, Proceedings of the European Peptide Symposium* (Eds.: G. Jung, E. Bayer), de Gruyter, Berlin, **1989**, pp. 37–39; c) L. A. Carpino, *J. Am. Chem. Soc.* **1993**, *115*, 4397–4398; d) L. A. Carpino, A. El-Faham, C. A. Minor, F. Albericio, *J. Chem. Soc. Chem.Comm.* **1994**, 201–203; e) J. C. H. M. Wijkmans, J. A. W. Kruijtzer, G. A. van der Marel, J. H. van Boom, W. Bloemhoff, *Recl. Trav. Chim. Pays-Bas* **1994**, *113*, 394–397; f) L. A. Carpino, A. El-Faham, F. Albericio, *J. Org. Chem.* **1995**, *60*, 3561–3564; g) L. A. Carpino, A. El-Faham, *J. Am. Chem. Soc.* **1995**, *117*, 5401–5402; h) A. El-Faham, *Chem. Lett.* **1998**, 671–672; i) J. Habermann, H. Kunz, *J. Prakt. Chem.* **1998**, *340*, 233–239; j) P. Garner, J. T. Anderson, S. Dey, W. J. Youngs, K. Galat, *J. Org. Chem.* **1998**, *63*, 5732–5733; k) M. A. Bailén, R. Chinchilla, D. J. Dodsworth, C. Najera, *J. Org. Chem.* **1999**, *64*, 8936–8939; l) A. El-Faham, *Lett. Pept. Sci.* **2000**, *7*, 113–121; m) F. Albericio, M. A. Bailen, R. Chinchilla, J. D. Dodsworth, C. Najera, *Tetrahedron* **2001**, *57*, 9607–9613; n) O. Marder, Y. Shvo, F. Albericio, *Chim. Oggi* **2002**, *20*, 37–41; o) M. Vendrell, R. Ventura, A. Ewenson, M. Royo, F. Albericio, *Tetrahedron Lett.* **2005**, *46*, 5383–5386.

[7] a) A. El-Faham, F. Albericio, *Org. Lett.* **2007**, *9*, 4475–4477; b) A. El-Faham, F. Albericio, *J. Org. Chem.* **2008**, *73*, 2731–2737.

[8] I. Abdelmoty, F. Albericio, L. A. Carpino, B. F. Foxman, S. A. Kates, *Lett. Peptide Sci.* **1994**, *1*, 57–67.

[9] a) L. A. Carpino, H. Imazumi, A. El-Faham, F. J. Ferrer, C. Zhang, Y. Lee, B. M. Foxman, P. Henklein, C. Hanay, C. Mügge, H. Wenschuh, J. Klose, M. Beyermann, M. Bienert, *Angew. Chem.* **2002**, *114*, 457–461; *Angew. Chem. Int. Ed.* **2002**, *41*, 441–445.

[10] K. D. Wehrstedt, P. A. Wandrey, D. Heitkamp, *J. Hazard. Mater.* **2005**, *126*, 1–7.

[11] R. Subirós-Funosas, R. Prohens, R. Barbas, A. El-Faham, F. Albericio, *Chem. Eur. J.* **2009**, DOI: 10.1002/chem.200900614.

[12] G. Breipohl, W. Koenig, *Ger. Offen.* DE 90-4016596, **1991**.

[13] L. A. Carpino, P. Henklein, B. M. Foxman, I. Abdelmoty, B. Costisella, V. Wray, T. Domke, A. El-Faham, C. J. Mugge, *Org. Chem.* **2001**, *66*, 5245–5247.

[14] R. King, R. Hirst, *Safety in the Process Industries*, 2nd ed., Elsevier, Oxford, **2002**.

[15] J. Steinbach, *Safety Assessment for Chemical Processes*, Wiley-VCH, Weinheim, **1999**, pp. 29–46.

[16] F. Stoessel, *Thermal Safety of Chemical Processes*, Wiley-VCH, Weinheim, **2008**, 311–334.

[17] I. Townsend, *J. Therm. Anal.* **1991**, *37*, 2031–2066.

[18] a) F. Stoessel, *Chem. Eng. Prog.* **1993**, *89*, 68–75; b) F. Stoessel, H. Fierz, P. Lerena, G. Killé, *Org. Proc. Proced. Int.* **1997**, *1*, 428–434.

[19] a) T. C. Hofelich, R. C. Thomas, *Int. Symp. Runaway React.* **1989**, 74–85; b) J. Singh, C. Simms, *Inst. Chem. Eng. Symp. Ser.* **2001**, *148*, 67–79.

[20] J. Barton, R. Rogers, *Chemical Reaction Hazards*, 2nd ed., Institution of Chemical Engeneers, Rugby (UK), **1997**.

[21] M. Kitamura, S. Chiba, K. Narasaka, *Bull. Chem. Soc. Jpn.* **2003**, *76*, 1063–1070.

↖↖ These are not the final page numbers!

[22] K. N. F. Shaw, C. Nolan, *J. Org. Chem.* **1957**, *22*, 1668–1670.

[23] J. Izdebski, *Pol. J. Chem.* **1979**, *53*, 1049–1057.

[24] A. El-Faham, S. N. Khattab, M. Abdul-Ghani, F. Albericio, *Eur. J. Org. Chem.* **2006**, 1563.

[25] P. F. Wiley, Hsiung Verónica, *Spectrochim. Acta Part A* **1970**, *26*, 2229–2230.

[26] A. El-Faham, *Org. Prep. Proced.* **1998**, *30*, 477–481.

[27] B. Roduit, W. Dermaut, A. Lungui, P. Folly, B. Berger, A. Sarbach, *J. Therm. Anal.* **2008**, *93*, 163.

These are not the final page numbers! ↗↗

Peptide Synthesis ————————

A. El-Faham,* R. S. Funosas,
R. Prohens, F. Albericio* . . . ▮▮▮▮–▮▮▮▮
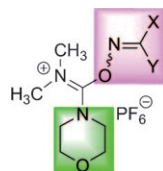
🖥 **COMU: A Safer and More Effective Replacement for Benzotriazole-Based Uronium Coupling Reagents**

Uronium coupling reagents: A new family of uronium-type coupling reagents differing in their iminium moieties and leaving groups (see Figure) is described. The presence of the morpholino group in combination with an oxime derivative, especially ethyl 2-cyano-2-(hydroxyimino)acetate (Oxyma), had a marked influence on the solubilities, stabilities, and reactivities of the reagents. Furthermore, the Oxyma moiety offers a lower explosion risk than benzotriazole derivatives.